International Journal of
INTELLIGENT SYSTEMS AND APPLICATIONS IN ENGINEERING
ISSN:2147-6799 www.ijisae.org Original Research Paper

Performance Analysis of Induction Motor Drive System using Alternate Arm Converter and Modular Multilevel Converter- A Comparison

S.T.Rama[1,2,*], V.Rajini[3]

Submitted: 22/10/2023 **Revised**: 16/12/2023 **Accepted**: 22/12/2023

Abstract: The Modular Multilevel Converter (MMC) and Alternate Arm Converter (AAC) have gained significant popularity in High voltage direct current (HVDC) transmission systems due to their versatile advantages such as modularity, scalability, DC fault tolerance, harmonic distortion mitigation, controllability, improvement in quality of power, high efficiency, etc. This paper presents a comprehensive study on developing a nine level Full bridge AAC based on the design principles of MMC, along with a detailed analysis of their configurations and performance characteristics. To facilitate a thorough comparison between MMC and AAC configurations, spectral analysis was conducted using various pulse width modulation (PWM) techniques including Level Shift, Phase Shift, Nearest Level Control (NLC), and Third Harmonics Injection (THI). The results highlight that a nine-level AAC with phase shift PWM technique exhibits the least total harmonic distortion when compared to other modulation techniques. Specifically, a nine-level MMC and AAC interfaced with an Induction Motor are designed and simulated in MATLAB/Simulink. Through simulation and analysis, this research aims to evaluate the performance of AAC in controlling the electric motor drive systems.

Keywords*: Modular Multilevel Converter, Alternate Arm Converter, Induction Motor, Pulse Width Modulation techniques, Voltage Stress.*

1. Introduction:

Power electronic converters play a crucial role in modern power systems, enabling efficient and reliable transmission and distribution of electrical energy. In the realm of high voltage applications, such as High Voltage Direct Current (HVDC) and High Voltage Alternating Current (HVAC) systems, the Modular Multilevel Converter (MMC) and Alternate Arm Converter (AAC) have emerged as the latest forerunners. The MMC and AAC have gained significant traction due to their distinct advantages over traditional multilevel voltage source converters (VSCs) [1]. The MMC, in particular, offers a modular and scalable topology, with series-connected sub-modules comprising power semiconductor devices and capacitors. This architecture allows for the generation of staircase voltage waveforms with small voltage steps, resulting in improved voltage waveform quality and reduced current distortion. Additionally, the MMC eliminates the need for bulky AC filters, reducing the physical footprint of converter stations and enhancing overall system efficiency [2]. Similarly, the AAC, derived from the design principles of the MMC, offers further advancements in high voltage converter technology. With its enhanced features and flexibility, the AAC is being increasingly implemented in HVDC and HVAC systems, as well as various applications in telecommunications, railway traction, data communication, and more. While the MMC and AAC have proven their effectiveness in high voltage applications, their potential in low and medium voltage applications has also garnered attention [3]. These converters can be seamlessly integrated into control systems for electric motor drives, pumps, blowers, fans, and other industrial applications [4]. The modular and scalable nature of the MMC and AAC enables their deployment across a wide range of voltage levels, making them suitable for various low, medium, and high voltage applications.

The following are the main contributions of the research work

a. The topologies of the Modular Multilevel Converter (MMC) and Alternate Arm Converter (AAC) with nine levels using full bridge configurations were designed and analysed based on the switching characteristics of IGBT switches.
b. A comparative spectral analysis on a nine level was performed on the Modular Multilevel Converter (MMC) and Alternate Arm Converter (AAC) models based on different pulse width modulation (PWM) techniques.
c. A comparative analysis was conducted to assess the speed control performance of an induction motor using both the Modular Multilevel Converter (MMC) and Alternate Arm Converter (AAC) across various loading conditions.

[1]*Research Scholar, Department of EEE, Sathyabama Institute of Science and Technology, Jeppiaar Nagar, Chennai, Tamilnadu, India.*
[2]*Assistant Professor, Dr.M.G.R Educational and Research Institute, Maduravoyal, Chennai, Tamilnadu, India. *Corresponding Email: rama.eee@drmgrdu.ac.in*
Orchid id - 0000-0002-1767-4082
[3]*Professor, Department of EEE, SSN College of Engineering, Kalavakkam, Tamilnadu, India.*

The paper is structured into several sections to present a comprehensive study on the design and performance analysis of MMC and AAC. In Section 2, a literature survey is conducted to gather relevant information and insights from previous research and studies in the field. Section 3 focuses on the system model, where the overall configuration and components of the MMC and AAC systems are described. Section 4 presents the detailed design methodology of MMC and AAC. In Section 5, a spectral analysis is performed based on different Pulse Width Modulation (PWM) techniques. Following that, the voltage stress analysis is conducted for MMC and AAC in Section 6. Section 7 involves the performance analysis and simulation results of an induction motor interfaced with MMC and AAC. Finally, in Section 8, a concise conclusion is drawn based on the findings.

2. Literature Survey:

The literature survey conducted for this research work focused on gathering relevant studies and publications related to the MMC and AAC. In [5], investigates the interoperability of the AAC with the MMC in a hybrid VSC-HVDC system. It showcases the AAC's performance in terms of interoperability and control functions using an 800 MVA hybrid VSC-HVDC system. The study validates the AAC's effectiveness in complex hybrid DC grid configurations and practical HVDC systems. In [6] proposes the use of the AAC as an alternative to the MMC for medium voltage adjustable speed drive applications. The AAC offers advantages such as lower energy storage requirements and reduced device count. The paper investigates the energy requirements of the AAC for different load characteristics and validates the findings through simulations and experiments. In [7], compares HVDC converters, specifically the modular multilevel and alternate arm converter topologies, with a focus on power quality, losses, and design parameters. The findings highlight the advantages of the mixed cell modular converter in terms of power losses, power quality, and control range. However, reducing the number of cells per arm and operating at high voltage may have negative impacts on switching losses and power quality at the DC side. In [8], proposes a time-sharing principle-based modular multilevel converter (TS-MMC) for medium- to high-voltage power transmission. The TS-MMC combines cascaded switch stacks (CSSs) and AACs to achieve a lightweight design and improved efficiency. It reduces the number of sub-modules (SMs) required and enables DC fault blocking capability. The feasibility of the TS-MMC is validated through mathematical models, control strategies, and simulation/experimental results. In [9], compares the MMC and AAC for high-power industrial applications. It evaluates their modularity, scalability, and reliability in HVDC systems. Through performance analysis and numerical simulations using Matlab/Simulink, the study highlights the advantages of each converter. The focus is on their performance when supplying a passive inductive load.

In [10], presents a new modulation technique called windowed pulse width modulation (W-PWM) for modular multilevel converters in variable speed traction drives. W-PWM combines the strengths of existing MMC modulation schemes, offering reduced switching losses and lower current harmonic distortion. The technique allows for dynamic performance optimization based on operating conditions and demonstrates promising results through simulations and experiments. In [11], presents a new medium-voltage AC-AC modular multilevel converter with advantages in size, weight, cost, and operational performance compared to traditional converters. It addresses limitations of high-voltage ripples and unbalanced grid conditions. The converter has a simple structure, requires fewer control loops, and eliminates the need for arm inductors. Simulation and experimental results validate its performance for machine-drive applications like offshore wind turbines.

In [12], compares the performance of conventional Direct Torque Control (DTC) with Neutral Point Clamping (NPC) and DTC with MMC for driving an Induction Motor (IM). The aim is to address issues such as high torque and flux ripples, as well as speed reduction, through MATLAB/Simulation. In [13], introduces a driving system for a variable-speed induction machine-based MMC with magnetic channels. It addresses the issue of high voltage ripple in submodule capacitors at low speeds by utilizing dual half-bridge modules. The system achieves a significant reduction in voltage ripple compared to previous works and employs field-oriented control (FOC) for efficient motor operation. The system design is validated using MATLAB/Simulink simulations.

There is a lack of comprehensive and comparative studies that specifically focus on the performance characteristics, advantages, and limitations of AAC and MMC in the context of induction motor control. While AAC and MMC have been extensively studied and applied in various applications, there is a need for research that specifically investigates their performance when driving induction motors. Key aspects that should be addressed in this research include the dynamic response of AAC and MMC when controlling induction motors, their torque and speed control capabilities, power quality aspects such as harmonic distortion and voltage regulation, overall system efficiency, reliability, and their operational behaviour under different operating conditions, load characteristics, and control strategies. By conducting a thorough analysis and comparison of AAC and MMC in driving induction motors, researchers can identify the strengths and weaknesses of each converter topology and gain a better

understanding of their effectiveness, efficiency, and performance in motor control applications. This research would contribute to optimizing the design and control strategies of AAC and MMC for induction motor drives, leading to improved system performance and energy efficiency.

3.System Model

This system model provides a thorough investigation into the design, analysis, and development of an AAC based on the MMC design tenets. The Figure 1 shows the framework for speed control of induction motor using MMC and AAC. The first part of this paper examines the configurations and design concepts of both MMC and AAC converters, with an emphasis on the modularity and scalability of these devices. Following that, PWM techniques like level Shift, Phase Shift, Nearest Level Control (NLC), and Third Harmonic Injection (THI), are employed to generate the switching pulses to trigger the IGBT switches in the converters. A spectrum analysis on the output voltage is performed to provide a complete comparison of MMC and AAC systems.

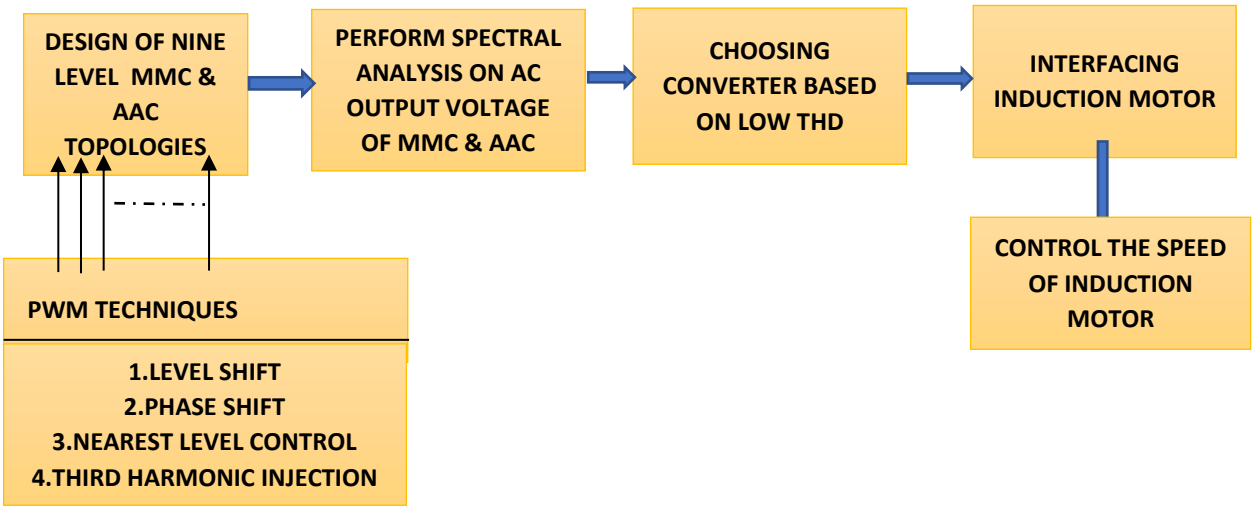

Fig 1: Block Diagram of System Model

The study focuses on selecting the converter which exhibits low total harmonic distortion. The induction motor is connected to the selected converter (both MMC and AAC) with low THD and the performance of the induction motor is analysed while controlling the speed of the drive and the parameters which pertain in affecting the performance of the induction motor in connecting to the inverter is also dealt in the forthcoming sections.

4.Design of Mmc and Aac

In this section, the modelling of nine level Full bridge MMC and AAC is performed using MATLAB/Simulink. The N-level configurations of MMC and AAC are represented in Figure 2, providing a visual representation of the circuit connections and component arrangement. The design parameters for the MMC configuration are calculated using [14], which outlines the procedure for determining parameters such as the number of levels, capacitor values, and switching frequencies. Similarly, the design parameters for the AAC configuration are obtained using [15]. In order to achieve a low harmonic output voltage, various Pulse Width Modulation (PWM) techniques are employed. These techniques help in controlling the switching patterns of the MMC and AAC, leading to reduced harmonic distortion and improved output waveform quality. The selection of the appropriate PWM technique depends on factors such as system requirements, switching frequency, and desired harmonic performance.

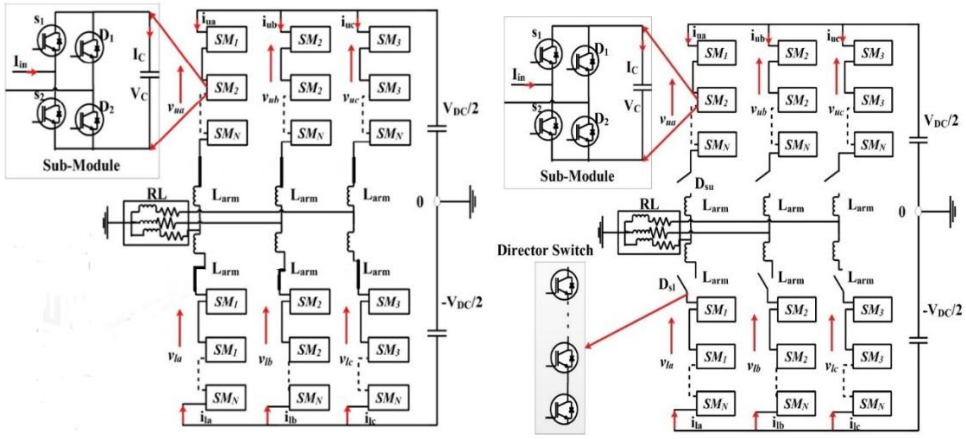

Fig 2. (a) Configuration of a N-level MMC and (b) Configuration of a N-level AAC

Table 1 provide the switching patterns required for proper operation of the nine-level MMC and AAC configurations, respectively. These patterns determine the activation and deactivation of the switches in the converter circuit, ensuring the desired output voltage levels and control of the current flow. By utilizing MATLAB/Simulink, the models of the MMC and AAC configurations can be simulated, allowing for analysis and evaluation of their performance characteristics.

Table 1: Switching Patterns for a nine level MMC and AAC

SM	OUTPUT PHASE VOLTAGE								
	Vdc	3Vdc/4	Vdc/2	Vdc/4	0	- Vdc/4	- Vdc/2	-3Vdc/4	-Vdc
SML1	0	0	0	0	0	0	0	0	1
SML2	0	0	0	0	0	0	0	1	1
SML3	0	0	0	0	0	0	1	1	1
SML4	0	0	0	0	0	1	1	1	1
SML5	0	0	0	0	1	1	1	1	1
SML6	0	0	0	1	1	1	1	1	1
SML7	0	0	1	1	1	1	1	1	1
SML8	0	1	1	1	1	1	1	1	1
SMU1	1	0	0	0	0	0	0	0	0
SMU2	1	1	0	0	0	0	0	0	0
SMU3	1	1	1	0	0	0	0	0	0
SMU4	1	1	1	1	0	0	0	0	0
SMU5	1	1	1	1	1	0	0	0	0
SMU6	1	1	1	1	1	1	0	0	0
SMU7	1	1	1	1	1	1	1	0	0
SMU8	1	1	1	1	1	1	1	1	0

5.Spectral Analysis Based on Pwm Techniques

Spectral analysis is used to investigate the frequency components of the output voltage waveform. This study aids in assessing the harmonic content and locating any undesirable frequency elements that can affect power quality.

a. Level Shift PWM:

The level shifted carrier pulse width modulation is seen in Fig. 3. To provide a uniform power distribution across the cells, each cell is separately modulated using sinusoidal unipolar pulse width modulation and bipolar pulse width modulation, respectively. For a cascaded inverter, a carrier level shift of 1/m (number of levels) is applied across the cells to provide a stepped multilevel output waveform with less distortion.

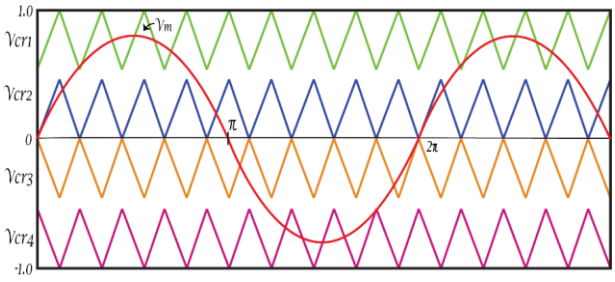

Fig 3. Level Shift PWM Technique

b. Phase Shift PWM:

The phase-shifted carrier pulse width modulation is seen in Figure 4. An uniform power distribution across the cells is achieved by separately modulating each cell using sinusoidal unipolar pulse width modulation and bipolar pulse width modulation, respectively. For a cascaded inverter, a carrier phase shift of 180°/m (number of levels) is applied across the cells to provide a stepped multilevel output waveform with less distortion.

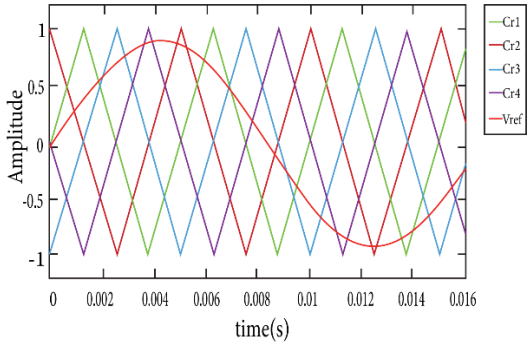

Fig 4. Phase Shift PWM Technique

c. Nearest Level Control (NLC) PWM:

NLC PWM chooses the voltage level that is closest to the reference signal to reduce switching losses. It may lead to reduced harmonics and better power quality. The Nearest Level Control PWM Technique is shown in Figure 5.

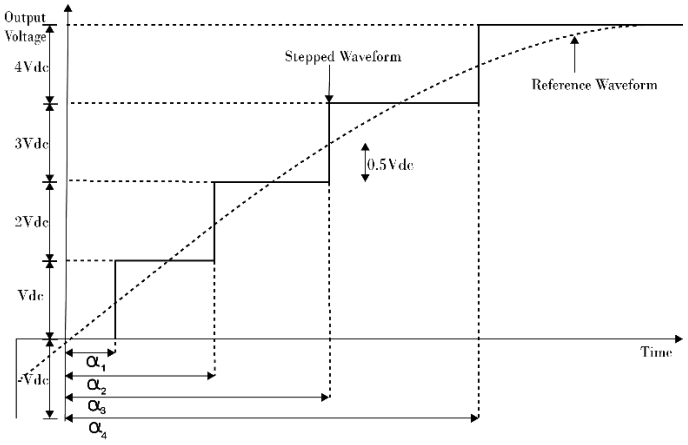

Fig 5. Nearest Level Control PWM Technique

d. Third Harmonics Injection (THI) PWM:

Although sinusoidal PWM is the easiest modulation strategy to grasp, it cannot completely use the DC bus

supply power. Third-harmonic injection pulse-width modulation (THIPWM) was created to increase inverter performance due to this issue. Maximum output voltage decreases with sinusoidal PWM. This study examines increasing maximum output voltage. Thus, adding a third harmonic signal to each reference signal increases output voltage amplitude without affecting quality, as seen in Figure 6.

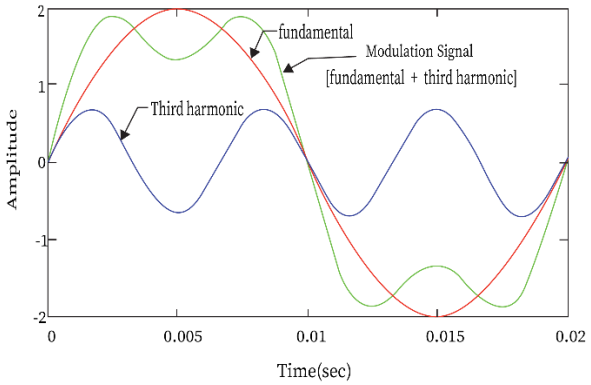

Fig 6. Third Harmonics Injection (THI) Technique

Both converters are subjected to each PWM approach, and the resultant frequency spectra are examined and contrasted. The effectiveness of each setup and PWM approach is assessed using THD value.

Table 2 provides a comparative analysis of different PWM techniques used in both MMC and AAC configurations. The analysis focuses on the harmonic distortion present in the output voltage waveform for each techni0que.

Table 2: Comparative analysis PWM techniques in MMC and AAC

PWM Techniques	THD for Nine Level Full Bridge MMC (%)	THD for Nine Level Full Bridge AAC (%)
Level Shift PWM	**17.67**	**17.05**
Phase Shift PWM	**14.12**	**13.26**
Nearest Level Control	**14.88**	**13.93**
Third Harmonic Injection	**16.53**	**17.24**

Based on the analysis, the table 2 indicates that both MMC and AAC configurations incorporating phase shift PWM technique generates the least percentage of total harmonic distortion in the output voltage when compared to other PWM techniques. On the other hand, implementing level shift PWM technique in the converter configuration records the highest THD among the other designs adopting different PWM techniques. The comparative analysis provided in Table 2 helps in optimizing the performance of the converters and achieving improved waveform quality in high voltage DC systems.

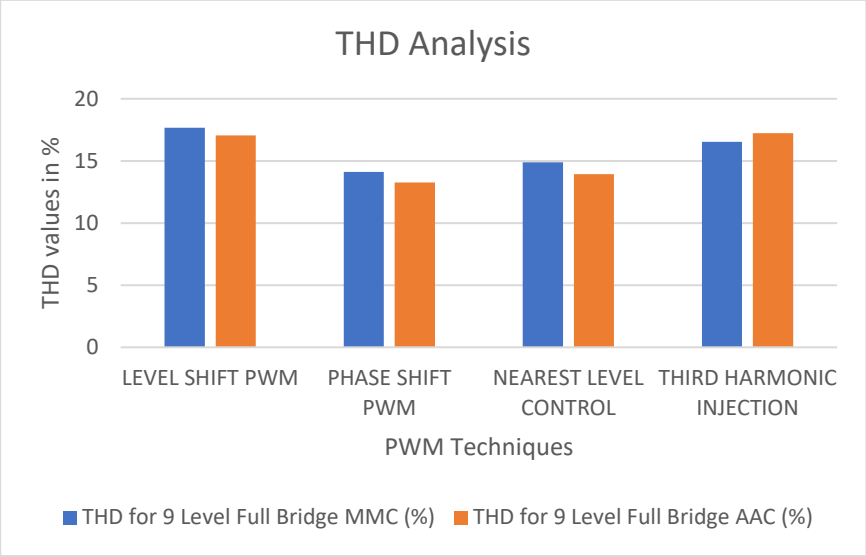

Fig 7. Comparative Analysis of output voltage of Full Bridge MMC and AAC based on THD values

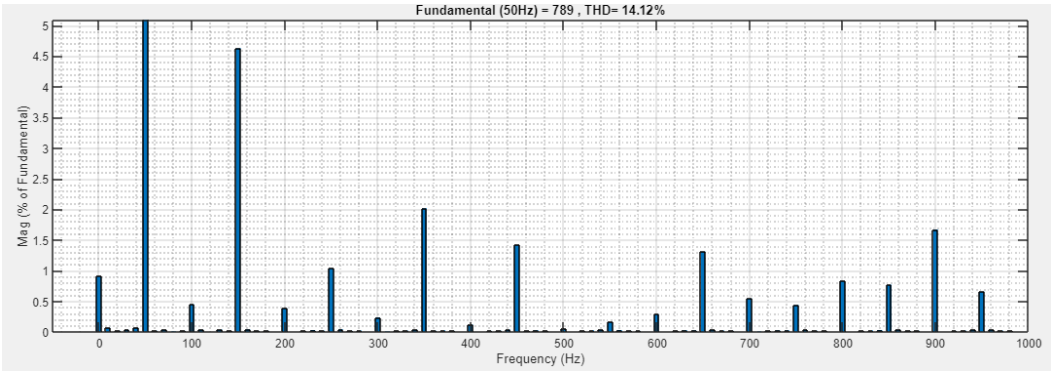

Fig 8. Spectral Analysis of output voltage of Full Bridge topology of a Nine Level MMC

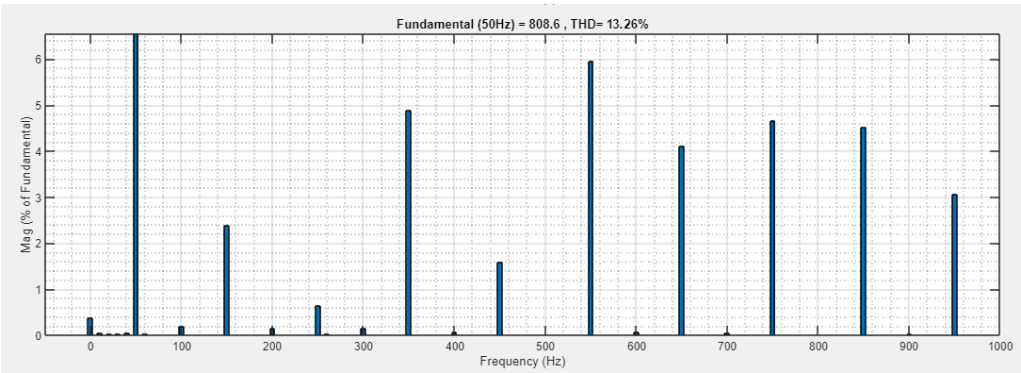

Fig 9. Spectral Analysis of output voltage of Full Bridge topology of a Nine Level AAC

The figure 7 illustrates the graphical representation of the comparative analysis of output voltage of Full Bridge MMC and AAC based on THD values. The figures 8 and 9 depicts the THD values for each converter configuration, allowing for a comparison of their low harmonic distortion levels.

6. Voltage Stress Analysis in Mmc and Aac

This section discusses about the voltage analysis in MMC and AAC. The voltage stress in converters refers to the increasing voltage levels encountered by components inside a converter circuit, which often result in adverse impacts on their performance and dependability. This stress arises from high-frequency switching events, inductive loads causing back EMF, parasitic elements inducing unexpected oscillations, overvoltage conditions exceeding converter ratings, and rapid load fluctuations, collectively stressing components like IGBTs and diodes.

In a typical nine-level full bridge MMC or AAC configuration, each system comprises of eight submodules, with each submodule consisting of four IGBT switches. After applying an input voltage of +/- 400V to both the MMC and AAC systems, an AC output voltage of 800V is obtained across the load. Hence, the

voltage drop across the IGBT switches is determined, with an approximated value of 200V per IGBT switch. However, the measured voltage drop across the IGBT switches differs between MMC and AAC. In MMC, the voltage drop was between 205-210V, whereas in AAC, it ranged from 198-200V which is shown in Figure 10(a) and 10(b).

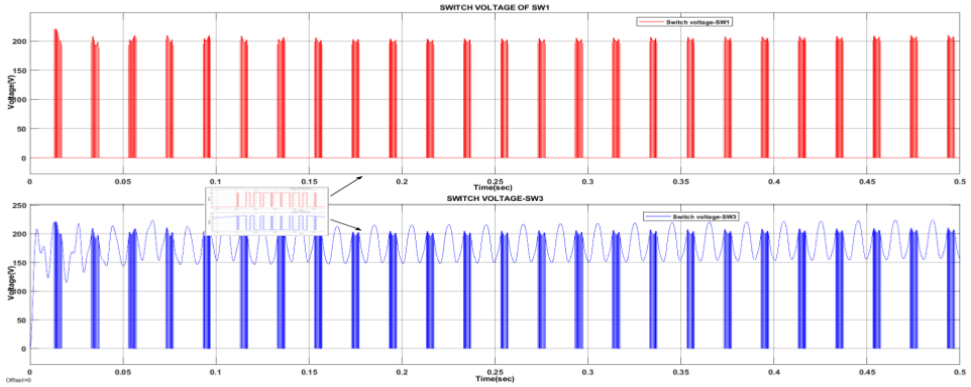

Fig.10 (a) Voltage stress of switch 1 and switch 3 of a MMC submodule

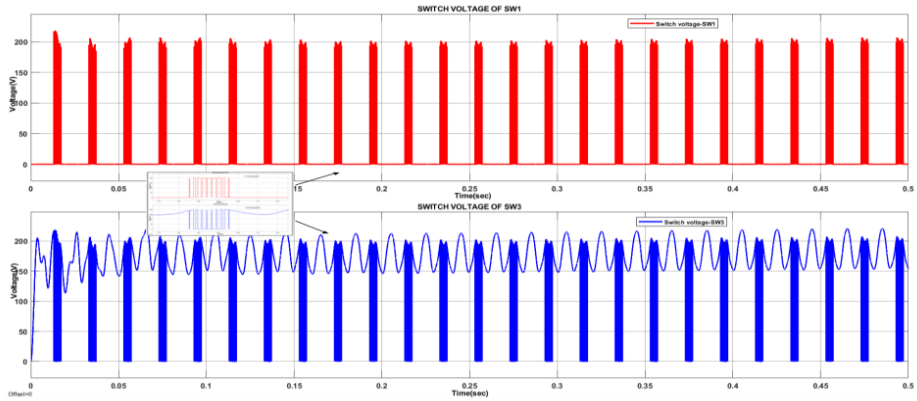

Fig.10 (b) Voltage stress of switch 1 and switch 3 of a AAC submodule

In MMC, a continuous current flow through all the submodules to produce positive and negative voltage cycles. However, this can strain the switches, causing power loss and reducing efficiency. The AAC configuration addresses this by activating only necessary submodules that contribute to the output voltage. This control is managed by specific switches, using fewer switches than the MMC. This reduction in switches in AAC significantly cuts power loss and stress on the switches. As a result, AAC is more efficient than MMC.

7. Performance Analysis of Induction Motor in Mmc and Aac

The paper explores the interfacing of an induction motor with both the MMC and AAC. The goal is to assess the characteristics of these converters in controlling electric motor drives. By connecting the induction motor to the MMC and AAC converters with various load conditions, the parameters of the induction motor like rotor speed, electromagnetic torque (T_e), rotor angle (Θ_m),stator currents(i_{sa}, i_{sb}, i_{sc}) and rotor currents(i_{ra}, i_{rb}, i_{rc}) are analysed and discussed in this section. The design parameters of MMC, AAC is provided in table 3.

Table 3: Design parameters of MMC and AAC

Parameter	MMC Specifications	AAC Specifications
DC voltage (Vdc)	+/-400V	+/-400V
Converter AC voltage (Vac)	800V	800V
Arm inductor (Lu& Ll)	4mH	1200µH

Arm resistance (Ru& Rl)	0.1Ω	0.1Ω
Cell capacitance (Ccell)	3000μF	350μF
No.of cell in arm (Ncell)	9	9
No. of series Director Switch (Ndir)	1	1
Switching Frequency (fs)	2kHz	2kHz

7.1 Interfacing the Induction motor with MMC and AAC

The performance of the induction motor is analysed based on various parameters by feeding the motor with AC input voltage from MMC and AAC. The motor is analysed on various load conditions like no load or minimum load, half, quarter and full load. The design parameters of Induction motor is provided in table 4.

Table 4: Design parameters of Induction motor

Parameter	Specifications
Rated Shaft Torque	23.746 N-m
Output Power	3730 W
Input Voltage (Vrms)	460V
Rated speed	1500 RPM
Frequency	50Hz
Stator Resistance and Inductance	1.115 Ω ,0.005974 H
Rotor Resistance and Inductance	1.083 Ω , 0.005974 H
No. of poles	4
Inertia, friction factor	0.02 0.005752 N.m.s
Mutual Inductance (Lm)	0.2037 H

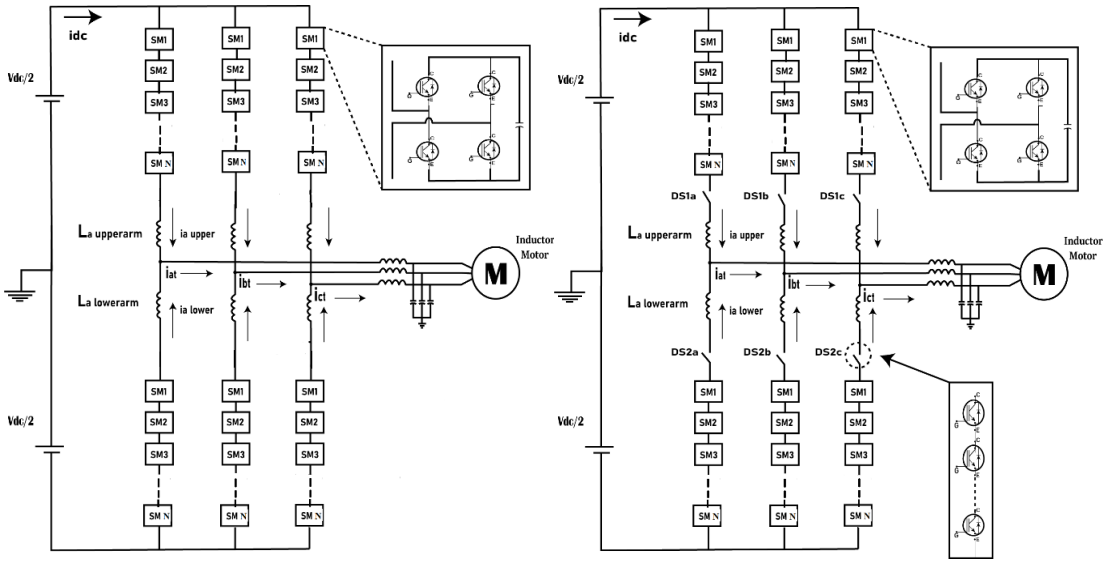

(a) (b)

Fig 11. (a) MMC interfaced with Induction motor (b) AAC interfaced with Induction motor

A three phase nine level MMC and AAC are interfaced with three phase induction motor to feed a pure sinusoidal AC input to the motor which is shown in Figure 11 (a) and (b). The analysis is performed to control the speed of the motor with and without adopting PI controllers and under different load conditions.

7.2 At Full load condition without PI Controller:

When operating the motor without controllers at full load conditions, the simulation results in figure 12 (a) show that the rotor speed of the motor interfaced with MMC fluctuates rapidly and reaches a speed of 1420 rpm at 0.18 seconds, which is 6% lower than the rated speed. Then in figure 12 (b), the motor interfaced with AAC also experiences speed fluctuations but settles down quickly at 1467 rpm. The electromagnetic torque (Te) generated by the motor interfaced with MMC is 24.5 N-m, with a stator current of 12.97 and rotor current of 11.1A. In contrast, the motor interfaced with AAC generates an electromagnetic torque of 24.63 N-m, with a stator current of 13.1A and a rotor current of 11.8 A.

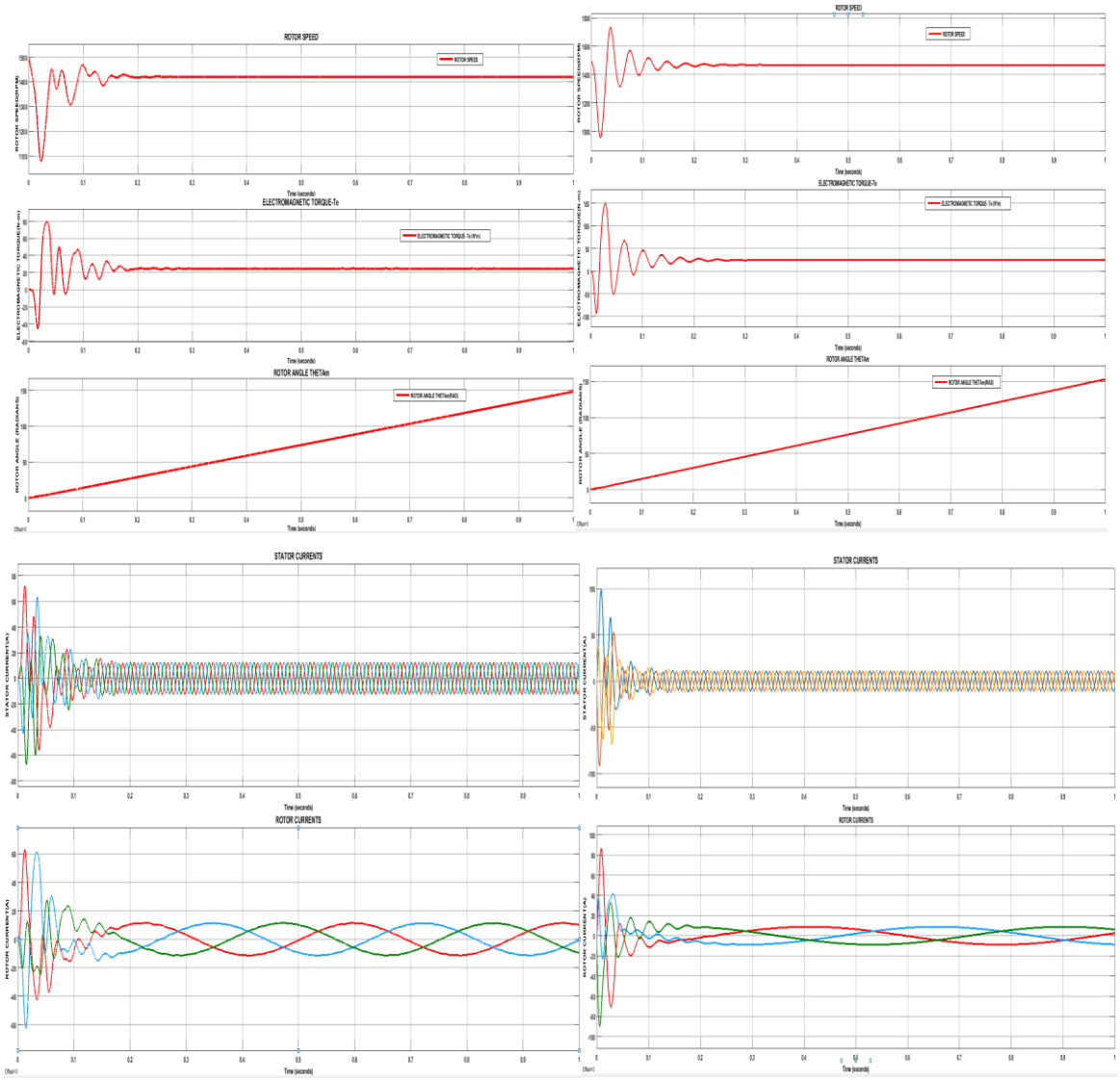

(a) (b)

Fig 12 (a) and (b): Rotor speed, Electromagnetic Torque and Rotor angle, Rotor and Stator currents of Induction motor interfaced with MMC and AAC

7.3 At Full Load Condition with PI controller:

In this paper, importance is imparted on the performance analysis of controlling the speed of the induction motor. The rated speed of the induction motor is obtained by incorporating the conventional control strategy employing PI controllers in the design. The parameters of PI controllers for MMC and AAC is shown in table 5.

Table 5: Design parameters of PI controller

Parameter	MMC	AAC
K_p	1	0.1
Ki	10	1

The rated speed of 1500 rpm of the motor fed from AAC is attained faster than motor fed from MMC. The speed of the motor fed from MMC initially oscillates rapidly and then settles down to 1500 rpm at 0.25 seconds but the speed of the motor fed from an AAC initially oscillates but settles down faster at 0.15 seconds to the rated speed. From the table 5, the proportional gain (Kp) and integral gain (Ki) of the AAC is low when compared to MMC. Since the Kp and Ki values are set high in the PI controller to attain the rated speed may increase the burden on the converter system which result in oscillations and instability in case of MMC and reduce the performance of the converter.

Due to which the starting torque also varies and as the motor runs at synchronous speed the electromagnetic torque (Te) almost reaches zero in both the interfacing of induction motor with MMC and AAC but fluctuation is less in later interfacing at starting condition of the motor which is shown in Figure 13 (a) and (b). The stator current of 11.59A and rotor current of 9.7 A is induced in induction motor interfaced with MMC which is analysed and the stator current of 11.91A and rotor current of 10 A is generated in induction motor interfaced with AAC when run at minimum load condition.

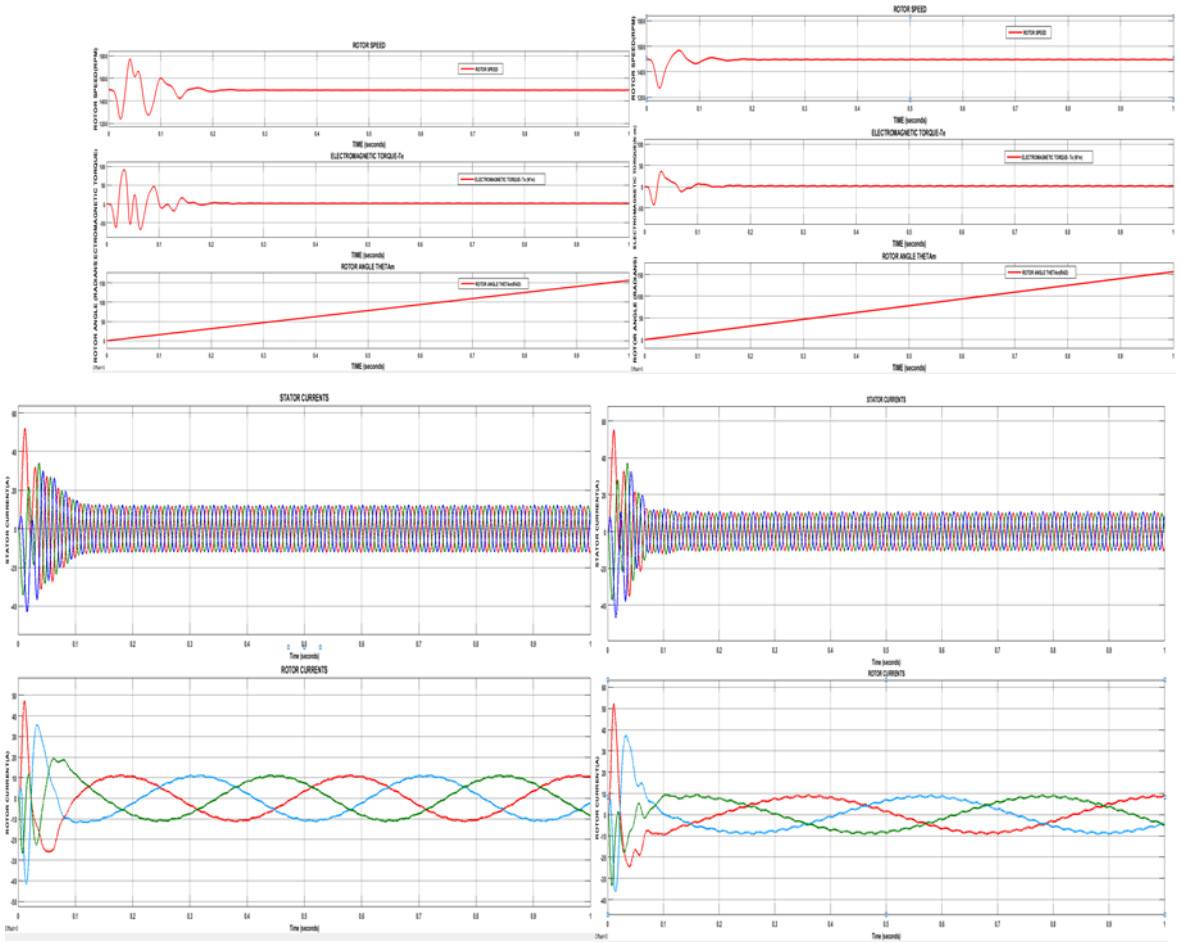

(a) (b)

Fig 13 (a) and (b): Rotor speed, Electromagnetic Torque, Rotor angle, Stator and Rotor currents of Induction motor interfaced with MMC and AAC

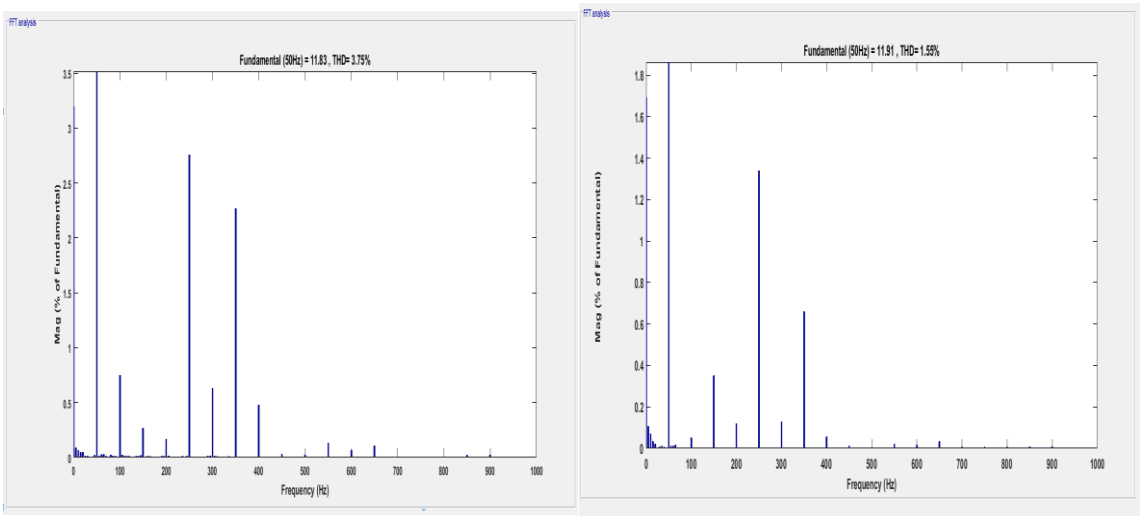

(a) (b)

Fig 14 (a) and (b): Spectral analysis of stator current of Induction motor interfaced with MMC and AAC

Spectral Analysis using Fast Fourier Transfer analysis is performed on the stator current of the induction motor interfaced with MMC and AAC which is represented in Figure 14 (a) and (b). The THD value for the stator current of induction motor interfaced with MMC is 3.75% and the THD value for stator current of induction motor interfaced with AAC is 1.55%. So, based on the above analysis the performance parameters of induction motor interfaced with AAC performs better than MMC due to few variations in the parameters which arises due to the different configurations of AAC and MMC, design parameters, operating conditions of the converters, different control strategies and applications, etc. Another analysis based on the loading of induction motor is also performed and a comparative discussion is put forth in this section. There are different types of torque influencing the operation of the motor. The gross mechanical or motor torque of induction motor is obtained by the total load or shaft torque imposed on the machine and torque losses due to windage, friction and iron losses. The torque losses are neglected when compared to the load torque.

7.4 At Various Load Conditions:

The Figure 15 (a) and (b) shows the Rotor speed(N), Electromagnetic torque(Te), Rotor angle(ϴm),Stator currents (isa,isb,isc) and rotor currents(ira,irb,irc) of Induction motor interfaced with MMC and AAC with various load conditions.

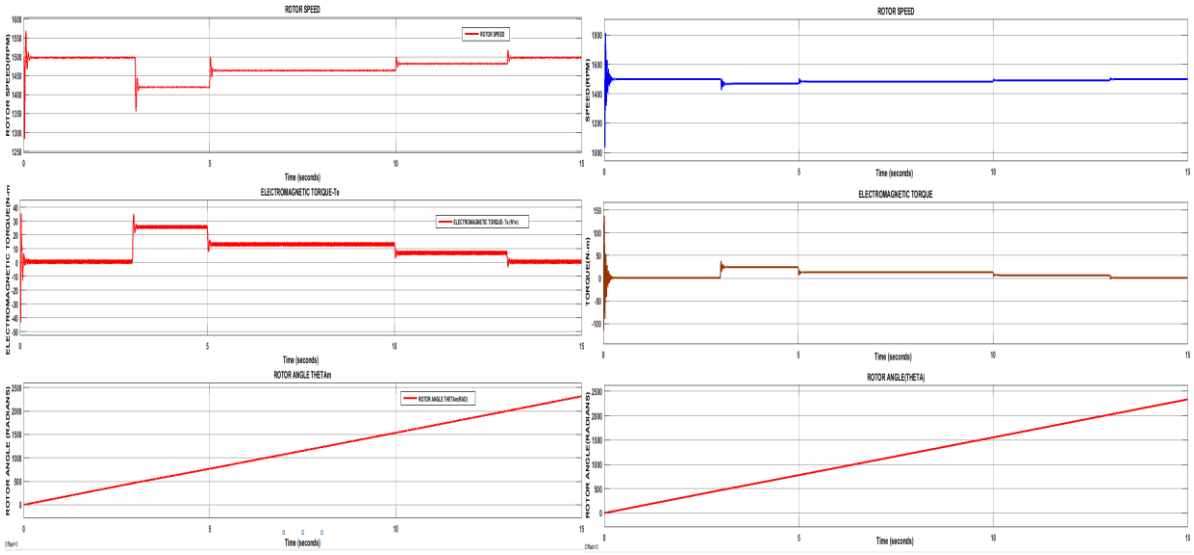

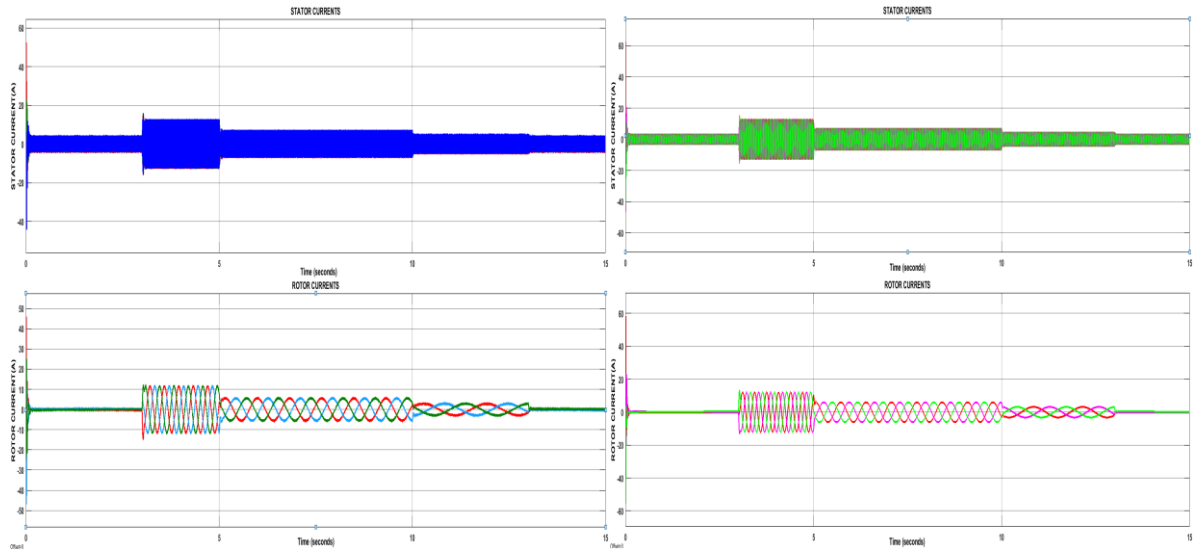

(a) (b)

Fig 15 (a) and (b): Rotor speed, Electromagnetic Torque, Rotor angle, Stator and Rotor currents of Induction motor interfaced with MMC and AAC with various loading

When the load on the induction motor (IM) is increased, the current also increases in order to deliver the required power of the IM and vice versa. When there is an increase in the slip(s) of the motor, obviously the speed of the motor based on equation 1 reduces to meet the additional power required and so the stator draws more power from the input source therefore, the stator current increases which in turn induces higher electromagnetic torque.

$$N = Ns(1 - s) \quad (1)$$

where N is the speed of the motor, Ns= Synchronous speed, s= slip.

As the load is withdrawn, there is a reduction in the input power as the need for output power is less or zero so the stator and rotor currents drawn by the motor reduces which is depicted in figures 14. The performance of induction motor is tested for full load, half load, quarter and no-load conditions when input voltage is fed from MMC and AAC. The motor torque and rotor speed for both the interfacing on different load conditions is summarized in table 6.

Table 6: Loading conditions on Induction motor

Load Torque(T_L) in N-m	Motor Torque N-m		Speed(N) in rpm	
	MMC	AAC	MMC	AAC
T_L at 3 secs	23.746	23.746	1420	1467
T_L at 5 secs	11.873	11.873	1465	1483
T_L at 10 secs	5.936	5.936	1480	1491
T_L at 13 secs	0	0	1500	1500

From the simulation results as depicted in figures 14, it has been analysed that initially the motor runs at 1500 rpm under no load condition till 3 seconds during which the Te is approximately 0.5N-m to 0.9N-m, stator current and rotor current is nearly 4.45A and 0.8 A for MMC interfacing and 3.59A,0.4A for AAC connection. From 3 seconds to 5 seconds, the motor is fully loaded with 23.746 N-m during which the Te, stator and rotor currents for MMC connection is 24.5N-m, 12.85A, 11A and as the motor is fully loaded the speed reduces to 1420 rpm whereas for AAC connection, Te is 24.63N-m, stator current is 13A and rotor current is 11.3A and speed of the motor reduces to 1467rpm. At 5 seconds, when the motor is half loaded, Te is12.4N-m, stator current is 7.2A and rotor current is 5.25A, motor speed increases to 1465 rpm for MMC. The Te is 12.765N-m, stator current is 7.12A and rotor current is 6A and speed increases to 1483 rpm for AAC interfacing. At 10 seconds, the motor is quarter loaded, motor speed increases to 1480 rpm, Te becomes 5.8 N-stator current 5.2A and rotor current of 2.5A for MMC interfacing and Te becomes 6.84N-m, stator current 4.8A and rotor current of 3.18A, motor speed reaches 1491 rpm for AAC interfacing. Finally, all the loads are withdrawn from the motor at 13 seconds leading the motor

to operate at rated speed for both the connection with Te to be approximately zero N-stator current of 4.47A and rotor current of 0.8A for MMC connection while stator and rotor current is 3.59 A and 0.42A for AAC interfacing are obtained. The harmonic components in the output voltage of MMC is more as compared to AAC leading to increase in the RMS value of stator current. This may result in higher copper loss of the motor and invariably affect the overall efficiency of the motor.

8. Conclusion:

The comparative analysis and simulation results of the MMC and AAC have demonstrated their potential and suitability for medium and low voltage level applications especially in the control of electric motor drives. The nine-level configurations of both converters, utilizing the phase shift PWM technique, proved to be effective in reducing total harmonic distortion (THD) and ensuring a cleaner power supply. The MMC and AAC exhibited distinct characteristics when interfaced with an induction motor. The MMC-connected motor experienced fluctuations in rotor speed, settling at 1420 rpm, slightly below the rated speed. In contrast, the AAC-connected motor demonstrated faster settling and achieved a stable speed of 1467 rpm without controllers. The analysis of electromagnetic torque, stator current, and rotor current further highlighted the differences between MMC and AAC. The MMC-generated torque was 24.5 N-m, with stator and rotor currents of 12.97A and 11.1A, respectively. The AAC-generated torque was 24.63 N-m, with stator and rotor currents of 13.1 A and 11.8 A, respectively. The controllers are included in the design to control the speed of the motor to operate it at rated speed. These findings highlight the modularity, scalability, and ability of AAC to mitigate harmonic distortions, making them promising solutions for efficient and reliable performance in various applications. Further research and development can focus on optimizing their performance and exploring practical implementations in real-world systems.

References

[1] Nami, A., & Nademi, H. (2018). Modular multilevel converter (MMC) and its control. In *Control of Power Electronic Converters and Systems* (pp. 141-166). Academic Press.

[2] Hariri, R., Sebaaly, F., & Kanaan, H. Y. (2020, October). A review on modular multilevel converters in electric vehicles. In *IECON 2020 The 46th Annual Conference of the IEEE Industrial Electronics Society* (pp. 4987-1993). IEEE.

[3] Sun, P., Tian, Y., Pou, J., & Konstantinou, G. (2022). Beyond the MMC: Extended modular multilevel converter topologies and applications. *IEEE Open Journal of Power Electronics*.

[4] Li, G., & Liang, J. (2022). Modular multilevel converters: Recent applications [History]. *IEEE Electrification Magazine*, *10*(3), 85-92.

[5] Wickramasinghe, H. R., Sun, P., & Konstantinou, G. (2021). Interoperability of modular multilevel and alternate arm converters in hybrid HVDC systems. *Energies*, *14*(5), 1363.

[6] Karaka, N. R., Reddy, G. A., & Shukla, A. (2022, October). Performance Analysis of the Alternate Arm Converter for Electric Drive Applications. In *2022 IEEE Energy Conversion Congress and Exposition (ECCE)* (pp. 1-6). IEEE.

[7] Vozikis, D., Adam, G. P., Rault, P., Tzelepis, D., Holliday, D., & Finney, S. (2018). Steady-state performance of state-of-the-art modular multilevel and alternate arm converters with DC fault-blocking capability. *International Journal of Electrical Power & Energy Systems*, *99*, 618-629.

[8] Huang, M., Li, W., Zou, J., & Ma, X. (2023). Analysis and Design of a Novel Hybrid Modular Multilevel Converter with Time-Sharing Alternative Arm Converter. *IEEE Transactions on Industrial Electronics*.

[9] Bensiali, H., Khoucha, F., Benrabah, A., Belila, A., & Benbouzid, M. (2022). Comparative Analysis of Modular Multilevel Converters and Alternate Arm Converters for HVDC Applications. In *Artificial Intelligence and Heuristics for Smart Energy Efficiency in Smart Cities: Case Study: Tipasa, Algeria* (pp. 312-321). Springer International Publishing.

[10] De Simone, D., Tricoli, P., D'Arco, S., & Piegari, L. (2020). Windowed PWM: A configurable modulation scheme for modular multilevel converter-based traction drives. *IEEE Transactions on Power Electronics*, *35*(9), 9727-9736.

[11] Gontijo, G., Wang, S., Kerekes, T., & Teodorescu, R. (2020). New AC–AC modular multilevel converter solution for medium-voltage machine-drive applications: Modular multilevel series converter. *Energies*, *13*(14), 3664.

[12] Mudhavath, S. N., & Rao, G. S. Control of Modular Multilevel Converter Fed 3-Phase Induction Motor using DTC with PI Controller.

[13] Ali, E. A. K., & Hassan, T. K. (2022). Induction motor drive based on modular-multilevel converter with ripple-power decoupling channels. *Indonesian Journal of Electrical Engineering and Computer Science*, *26*(2), 675-688.

[14] Zygmanowski, M., Grzesik, B., & Nalepa, R. (2013, September). Capacitance and inductance selection of the modular multilevel converter. In *2013 15th European Conference on Power Electronics and Applications (EPE)* (pp. 1-10). IEEE.

[15] Merlin, M. M., & Green, T. C. (2015). Cell capacitor sizing in multilevel converters: cases of the modular multilevel converter and alternate arm converter. *IET Power Electronics*, *8*(3), 350-360.